

# Localization of Just Noticeable Difference for Image Compression

Guangan Chen<sup>1</sup>, Hanhe Lin<sup>2</sup>, Oliver Wiedemann<sup>3</sup>, Dietmar Saupe<sup>3</sup>

<sup>1</sup>Image Processing and Interpretation (IPI), imec research group at Ghent University, Belgium

<sup>2</sup>School of Science and Engineering, University of Dundee, United Kingdom

<sup>3</sup>Department of Computer and Information Science, University of Konstanz, Germany

**Abstract**—The just noticeable difference (JND) is the minimal difference between stimuli that can be detected by a person. The picture-wise just noticeable difference (PJND) for a given reference image and a compression algorithm represents the minimal level of compression that causes noticeable differences in the reconstruction. These differences can only be observed in some specific regions within the image, dubbed as JND-critical regions. Identifying these regions can improve the development of image compression algorithms. Due to the fact that visual perception varies among individuals, determining the PJND values and JND-critical regions for a target population of consumers requires subjective assessment experiments involving a sufficiently large number of observers. In this paper, we propose a novel framework for conducting such experiments using crowdsourcing. By applying this framework, we created a novel PJND dataset, KonJND++, consisting of 300 source images, compressed versions thereof under JPEG or BPG compression, and an average of 43 ratings of PJND and 129 self-reported locations of JND-critical regions for each source image. Our experiments demonstrate the effectiveness and reliability of our proposed framework, which is easy to be adapted for collecting a large-scale dataset. The source code and dataset are available at <https://github.com/angchen-dev/LocJND>.

**Index Terms**—Image quality assessment, just noticeable difference, JND-critical regions, crowdsourcing, distortion localization

## I. INTRODUCTION

The just noticeable difference (JND), also referred to as the difference threshold, is the minimum change in stimulus intensity required to produce a noticeable difference in sensory experience [1]. The JND has been widely applied in the multimedia domain, such as audio perceptual assessment [2]–[4] and watermarking [5]. It has also been used to determine the optimal compression level for images [6], [7] and videos [8]. For a given reference image, the picture-wise just noticeable difference (PJND) refers to the minimal level of its compressed version at which a viewer begins to perceive noticeable differences [7].

The PJND of an image can be determined through either subjective studies or estimated by objective methods, i.e., algorithms. While objective methods are required for real-time applications, subjective studies are the foundation for

collecting benchmark data for the development and evaluation of objective methods. The typical process for conducting subjective studies to collect PJND data involves three steps [6], [7], [9]–[11]. First, a set of pristine images is collected and encoded at different levels of distortion using one or more compression algorithms. Second, for each source image and each codec, a group of human observers checks for visible artifacts among the encoded images. Finally, a psychometric function is fitted to the collected data yielding the PJND threshold for each source and codec.

Several methods have been proposed to determine the PJND of a given image, which can be categorized based on the presentation of images for comparison. The most commonly used presentations include 1) displaying a reference image and a distorted image sequentially [8], [12], 2) displaying a reference image and a distorted image side-by-side [9], [10], [13], and 3) a sensitive method known as the flicker test, as adopted by an ISO/IEC standard [14]. In addition, these methods can be categorized in terms of search strategies for PJND identification, including standard binary search [13], relaxed binary search [10], and slider-based search strategy [15].

Typically, distortions at the PJND compression level are visible only in a few regions of the image [7]. We call these regions *JND-critical regions*. In other words, starting from the source image and decreasing the bitrate of the encoding, artifacts will first be noticed in these JND-critical regions. JND-critical regions collected from multiple observers can be combined to form a new kind of saliency map for a given image, referred to as the *JND-criticality map*.

Although understanding the impact of JND-critical regions on PJND detection could contribute to the improvement of image compression algorithms, existing subjective PJND assessment studies have not yet considered JND-critical regions [6], [7], [9]–[11]. To address this limitation, we combine PJND assessment with a procedure to determine JND-critical regions using a self-reported localization method. Observers first identify the PJND for a source image and the corresponding sequence of its compressed versions and then click on the image to indicate the JND-critical regions. Since each person’s visual system is unique, both the PJND and JND-critical regions are subject to variation between individuals. To ensure reliable results, it is necessary to collect data from a large number of observers. For each source image, the JND-criticality map is finally computed

by applying Gaussian blur to the aggregated self-reported locations as in [16]. To achieve our goals at a reasonable cost, we conducted our experiment through crowdsourcing.

Our main contributions can be summarized as follows:

- i. We introduce the concept of JND-critical regions, which widens the traditional approach to PJND assessment.
- ii. We propose a method to assess PJND and JND-critical regions jointly. It combines a flicker test with slider-based search and incorporates the self-reported localization method. Conducting the study through Amazon Mechanical Turk (AMT) renders it effective and cost-efficient. To the best of our knowledge, this is the first subjective study that collected both PJND and JND-critical regions.
- iii. We supply a new image dataset KonJND++, annotated with PJND ratings and JND-critical regions. It contains 300 source images, with corresponding distorted images obtained using the JPEG or BPG compression scheme. For each source image, an average of 43 PJND ratings and 129 clicked locations are provided.

## II. RELATED WORK

### A. PJND-based image datasets

Multiple PJND-based image databases [6], [7], [9]–[11] have been published in recent years. Jin *et al.* [6] conducted a subjective assessment experiment in the lab to collect PJND ratings for JPEG-encoded images. A reference image and a distorted image were presented side-by-side, and a bisection method was used to select the appropriate distorted image [17].

Shen *et al.* [11] created a PJND dataset for VVC-compressed images, also using a lab-based study with side-by-side presentation and standard binary search.

Lin *et al.* [7] proposed a crowdsourcing-based framework to efficiently conduct subjective PJND assessments. The authors used the flicker test [14] to enhance sensitivity and a slider-based adjustment method to speed up the experiment. As a result, the authors created the largest PJND dataset to date, KonJND-1k, consisting of 1,008 source images and their corresponding distorted images compressed using JPEG or Better Portable Graphics (BPG) compressions.

### B. Other relevant work

Jiang *et al.* [18] conducted a crowdsourcing experiment that captures human visual exploration behavior in task-free situations by recording mouse-tracking movements. Using a general-purpose mouse, rather than an eye-tracker, enabled the collection of a large-scale dataset with 10,000 images.

Hosu *et al.* [19] conducted crowdsourcing experiments for self-reported attention in image quality assessment (IQA) tasks using a simple point-and-click annotation method. Results compared to lab-based eye-tracking experiments indicated that using point-and-click method is accurate enough for collecting self-reported attention in IQA tasks via crowdsourcing.

Pergament *et al.* [20] introduced a tool that collects spatio-temporal importance maps of videos. Observers can adjust the

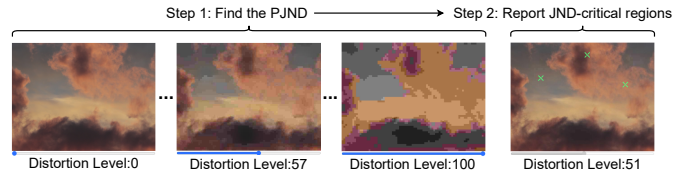


Fig. 1: Workflow for localizing JND-critical regions: Participants adjust a slider to find the PJND value (Step 1), followed by reporting three JND-critical regions (Step 2).

quality of a specific area of the video by annotating the map and the video stream displays the effects of the annotation. In a separate subjective study, the authors compared importance-map-generated videos with the encoded baseline using a two-alternative forced choice approach. The results showed that spatio-temporal importance map compressed videos were 1.9 times more preferred than traditionally compressed videos for a given bitrate.

## III. ASSESSMENT OF PJND AND LOCALIZATION OF JND-CRITICAL REGIONS

Our method to localize JND-critical regions proceeds in two steps, as shown in Fig. 1. The first step is to obtain the PJND value using the assessment method described in [7], where a reference image and its distorted version are displayed alternatively at a frequency of 8Hz [14]. This means the reference image appears (and disappears) four times per second, and while the reference is not shown, the distorted image is displayed instead at exactly the same location on the monitor.

The perceived amplitude of the resulting flicker effect depends on the image distortion. Participants use a slider to adjust the compression level such that they can *just* detect a flicker effect in at least three separate regions of the image. The slider position is mapped (details provided in VI) to the codec quality parameter such that the distorted images can easily be browsed in a sorted sequence.

After identifying their individual PJND thresholds, participants report the locations of three detected flickering regions by clicking on the image with their mouse. In our graphical user interface (GUI), a green cross indicates each clicked location for feedback.

## IV. IMAGE SAMPLING AND PILOT STUDY

Our images were sampled from the KonJND-1k dataset [7], which contains 504 source images compressed with JPEG and another 504 compressed with BPG. Also, all annotated PJNDs are provided in this dataset.

In a pilot study, we aimed to annotate 50 images that were used to generate ground truth for testing crowd worker attention in our main study. For each codec, we first sampled 25 images as “gold standard” images [23]. These images were to be used not only to educate crowd workers on the concepts of PJND and JND-critical regions but also to remove unreliable workers during the subsequent study questions. For this sampling, we sorted all 504 source images corresponding

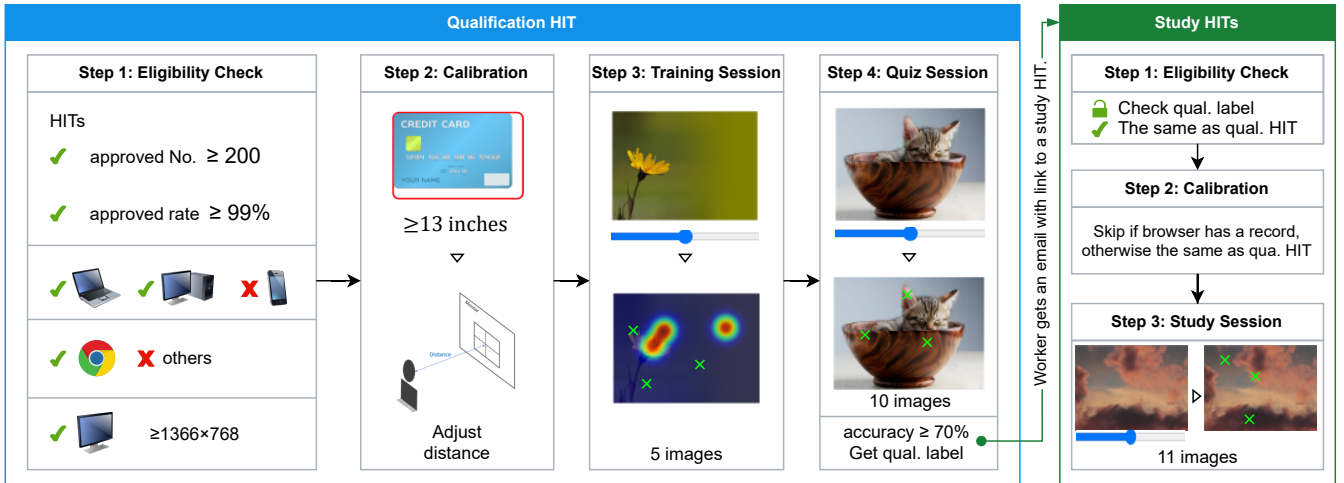


Fig. 2: The workflow of our study for JND-critical region localization. 1) **Qualification HIT**. Eligibility check: The study was only accessible to workers who had a positive record on AMT, and the GUI required that the worker’s device, browser, and screen resolution met the requirements. Calibration: To ensure all workers viewed the images at the same physical size, workers were required to place a payment card [21] on the screen and adjust a red frame until it fits the card size. The GUI then calculated the value of pixels per inch (PPI) based on the card and frame size and scaled the displayed images accordingly. After that, workers were asked to adjust their viewing distance to 30 cm [22]. Training and quiz session: To be eligible for study HITs, a worker must have completed a training session and passed a quiz to get a qualification label. 2) **Study HITs**. Workers could conduct the study HITs only if they had obtained their qualification labels and passed the eligibility check and calibration. A worker was allowed to participate in up to 20 study HITs.

to each codec with increasing PJND into 25 bins. From each of these bins, we selected the source image that showed the smallest variance of subjective PJNDs as this indicated better agreement on reported PJND values and, therefore, better suitability to test crowd worker attention.

For each codec in the main study, 150 images were sampled from the corresponding remaining 479 images in the KonJND-1k dataset. To ensure diversity in PJND values, we sorted the images in ascending order according to their mean PJND, then selected images at positions  $\lceil 479i/150 \rceil, i = 0, 1, 2, \dots, 149$ . In total, we arrived at  $2 \times (25 + 150) = 350$  images to be annotated in our crowdsourcing experiments.

## V. CROWDSOURCING JND-CRITICAL REGIONS

We conducted a main study on Amazon Mechanical Turk (AMT), a well-known crowdsourcing platform that allows to publish *human intelligence tasks* (HITs) to a large force of crowd workers. Fig. 2 shows the workflow. Similar to the KonJND-1k study, a quality control mechanism was introduced to ensure the collection of reliable PJND values.

The study consisted of a qualification HIT and multiple study HITs. The qualification HIT aimed to teach workers how to use the GUI and participate in the study. In the study HITs, we subsequently collect PJND ratings and JND-critical region annotations. Only participants that passed a quiz in the qualification HIT were allowed to contribute to the study HITs.

We followed the “gold standard” approach [23] with established ground truths to test the reliability of the participants.

The ground truths were derived from the annotated data of the pilot study. Details about generating ground truth for “gold standard” images are discussed in Section VI.

### A. Qualification HIT

While participating in the qualification HIT, workers were allowed to read the instructions on how to report the PJND value and JND-critical regions. To help illustrate the concept, an example was provided, showing three flickering regions. In the training session, if workers failed to report correct PJND or locations, they were shown the ground truths and required to repeat the assessment until their answers were correct. Participants were only allowed to report three locations if the reported PJND was within the acceptable range. The ground truth range of the PJND was displayed as text, and the ground truth JND-critical regions were depicted by a heat map, as shown in Fig. 2. After reporting correct PJND values and locations, workers moved on to the next image. We used five manually selected “gold standard” images for training.

In the quiz session, we required the workers to perform with an accuracy of 70% in order to be allowed to access study HITs. Accuracy was defined as

$$\text{accuracy} = \frac{b + c}{2a}, \quad (1)$$

where  $a = 10$  is the number of manually selected “gold standard” images in the quiz session,  $b$  is the number of

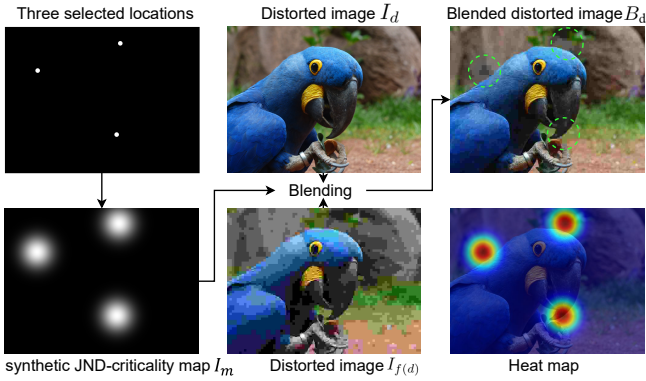


Fig. 3: Procedure of generating a blended distorted image  $B_d$  with three stronger distortion regions (green dotted circles).

correctly reported PJND values, and  $c$  is the number of images with at least two correctly reported locations.

We ran a script on our server to download the results from AMT in real-time and calculated the accuracy for each qualification HIT. Workers received a notification by email shortly after completion. Workers who passed the quiz received a link to a study HIT and were assigned an AMT qualification label. This was used as a token to participate in further study HITs.

### B. Study HITs

Once workers received their qualification label, they were allowed to conduct study HITs. Each study HIT had 11 images, ten of them were randomly selected from the source images (without replacement) and one was selected from the image set of the pilot study as a “gold standard” image. To ensure the PJND ratings were collected from a broad group of observers, workers were limited to completing up to 20 study HITs. The qualification label was revoked once a worker reached this limit.

The cumulative accuracy of a worker on “gold standard” images of completed study HITs was calculated by Eq. (1) in real-time. As each study HIT had one “gold standard” image,  $a$  was equal to the number of finished study HITs of the worker. After finishing 10 study HITs, workers whose cumulative accuracy was less than 70% were not allowed to continue, and their results were removed as outliers.

## VI. GROUND TRUTH GOLD STANDARD IMAGES

We monitored the attentiveness and compliance of our study participants by posing “gold standard” images. If their responses were considered unacceptable, their accuracy ratings decreased. The “gold standard” images and their distorted versions were constructed to establish well-defined criteria for acceptable responses regarding both the PJND rating and the JND-critical region localization.

To generate the ground truth range of acceptable PJND ratings, we followed the same procedures as developed in [7], where a sigmoid function with a randomly selected center is used to defined the expected PJND and the acceptable range

of PJND values. For brevity, we omit the details and refer the reader to the given reference.

To generate three clearly visible ground truth JND-critical regions for each “gold standard” test image, we selected their centers and locally increased the distortion level in their neighborhoods. To map distorted images into 100 distortion levels (corresponding to 100 slider positions), let  $I_d, d = 0, 1, \dots, 100$  denote the sequence of distorted images of a source image at distortion levels  $d$ . Thus, image  $I_0$  denotes the source image. For JPEG compression, image  $I_d, d > 0$  is compressed using JPEG’s quality factor (QF) equal to  $101 - d$ . For each distortion level  $d$  in the range of ground truth PJND, we defined a greater distortion level by  $f(d) = \lceil 80 + d/5 \rceil$ . As the quantizer parameters (QP) of BPG compression range from 1 to 51, to conveniently map QP values into 100 distortion levels, we only used QP values ranging from 1 to 50. A distorted image  $I_d, d > 0$  is compressed using QP equal to  $\lceil d/2 \rceil$ . In this case, we applied the function  $f(d) = \min\{\lceil 1.4d \rceil, 100\}$  to generate  $I_{f(d)}$ .

For  $d$  in the range of ground truth PJND, we blended images  $I_d$  with  $I_{f(d)}$ . The blending coefficients are defined by three image pixel locations  $(u_i, v_i), i = 1, 2, 3$  and  $\sigma = 35$  pixels. We let

$$w(x, y) = \frac{1}{c} \sum_{i=1}^3 \phi_{u_i, v_i, \sigma}(x, y),$$

where  $\phi_{u, v, \sigma}$  is the 2D standard normal distribution centered at  $(u, v)$  with variance  $\sigma^2$ , and  $c$  is a normalization constant such that the maximum of  $w$  is equal to 1. The blending function can be interpreted as a synthetic JND-criticality map. Then we summed the two images  $I_d$  and  $I_{f(d)}$ , weighted by  $1 - w$  and  $w$ , respectively. Fig. 3 illustrates the procedure.

We selected the locations of the ground truth JND-critical regions based on the JND-criticality maps from the self-reported locations in our pilot study. We identified the local maxima of the maps by the mean shift clustering method [24], and for each one, we computed the sum of pixel values in a  $7 \times 7$  window centered at the maximum. The three local maxima with the largest sums were selected as centers of the ground truth JND-critical regions.

In our experiment, each of the three synthesized JND-critical regions was considered covered by a mouse click of a study participant when the mouse pixel coordinates had a euclidean distance from the center  $(u_i, v_i)$  of the corresponding region of at most  $2\sigma$ . The overall response of a participant for the test image was considered correct if the chosen PJND was in the defined ground truth range and at least two of the three JND-critical regions were selected.

## VII. RESULT AND DISCUSSION

### A. Setup

Our main study contains 30 study HITs, where each HIT consists of 10 source images and one “gold standard” image. For each image, we collected assignments from 50 workers. In other words, 50 compound responses consisting of a PJND and three reported locations were collected for each image.

In total, we collected 16,500 responses, 15,000 for the study images and 1,500 for the “gold standard” test images.

### B. Outlier removal

In the study HITs, the reliability of the workers could not be fully assured even though they had passed the qualification quiz session. Some workers might have lost focus and attention during the experiment. Therefore, we followed the same procedures as used in the KonJND-1k study [7] to remove outliers at both the worker level and HIT level.

At the worker level, we identified and removed five workers who had a cumulative accuracy of less than 70% on “gold standard” images after completing 10 study HITs, indicating that they may have paid insufficient attention to the experiment. As a result, 540 responses from these workers were excluded, leaving a total of 14,460 responses.

At the HIT level, we filtered out results that deviated significantly from the mean PJND value and were inconsistent with the consensus of all workers. We applied the same method as in [7]. For each HIT, we removed 10% of the results, i.e., the results of 5 workers of a HIT were filtered out. As a result, a total of 12,960 responses remained.

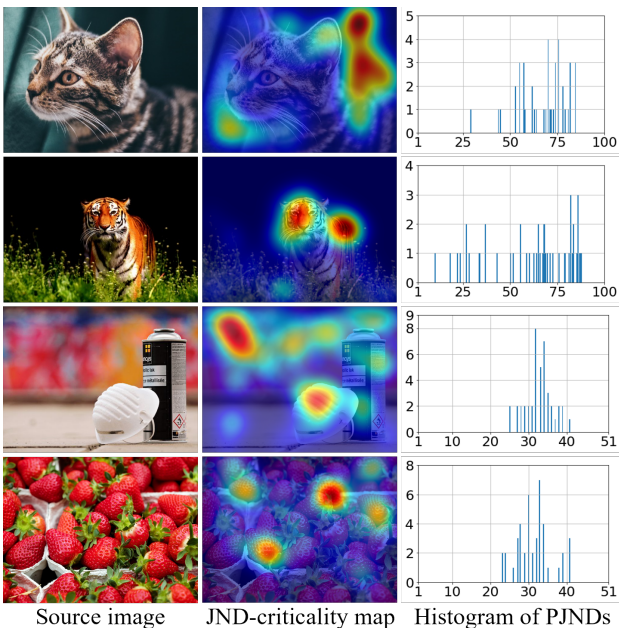


Fig. 4: Samples of the collected dataset in our study. The images in the first column were compressed by JPEG, JPEG, BPG, and BPG, respectively.

In addition, we excluded extreme PJND ratings that fell below 5 or exceed 95. As a result, the dataset consists of 300 source images with an average of 43 PJND values and 129 reported locations of JND-critical regions for each image. We named it the KonJND++ dataset. Fig. 4 shows four examples of the dataset.

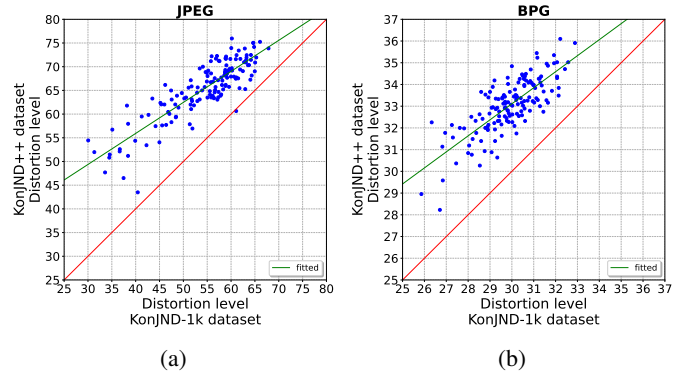


Fig. 5: A mean PJND values comparison between the KonJND++ dataset and KonJND-1k dataset on (a) JPEG compression and (b) BPG compression. Each dot represents the mean PJND values of a source image.

### C. Comparison of the KonJND++ and KonJND-1k datasets

To check for consistency with the KonJND-1k dataset, we compared the PJND samples of the KonJND++ dataset with those from the KonJND-1k dataset for the same 300 source images.

A scatterplot comparing the mean PJND values of images from both datasets is shown in Fig. 5. The regression lines for each compression method are

$$f(\bar{K}_I) = \begin{cases} 0.65\bar{K}_I + 29.73 & \text{for JPEG,} \\ 0.74\bar{K}_I + 10.97 & \text{for BPG,} \end{cases}$$

where  $\bar{K}_I$  denotes the mean PJND value of a reference image ( $I$ ) in the KonJND-1k dataset.

It is apparent that most of the mean PJND values from the KonJND++ dataset are higher than those from the KonJND-1k dataset. This difference is regarded as a natural bias. It is likely caused by the additional task in our study, requiring participants to report three flickering locations, which caused them to select larger distortion levels so they could perceive multiple flickering regions.

In addition, we computed the Spearman rank order correlation between the PJND values of the KonJND++ and those in KonJND-1k. The SROCC is 0.828 for JPEG compression and 0.740 for BPG. This high correlation indicates a good agreement between the two studies.

## VIII. DISCUSSION AND FUTURE WORK

In this paper, we present a framework for collecting PJND values and JND-critical regions, and we created a dataset named KonJND++ that consists of 300 source images. The framework is intended to collect large-scale datasets through crowdsourced experiments for training deep learning models, e.g. to predict JND-criticality maps for various applications.

JND-criticality maps could be combined with visual attention maps [18]. The JND-criticality map indicates regions with strong compression artifacts, while the visual attention map represents human attention with respect to the image contents.

Combining them may be beneficial for research on saliency-based compression, local quality prediction, or even foveated image and video coding [25]–[28].

A further subjective study is required to verify whether compressing the JND-critical regions less than other areas can improve perceived image quality at a given bitrate. This study can be a side-by-side flicker test where viewers are asked to select which side has a stronger flicker effect. On one side an adaptively compressed image with locally enlarged bitrate in the JND-critical regions alternates with the corresponding source image, and on the other side a standard compressed image with the same overall bitrate alternates with the source. If the flicker effect is stronger on the side with the standard compressed image, it will be confirmed that the JND-critical regions can improve image quality of compressed images.

## IX. CONCLUSION

We introduced the concept of JND-critical regions that may help in the development of perceptually guided image and video compression algorithms. We designed a PJND assessment method that involves collecting PJND using a flicker test with slider-based adjustment and collecting JND-critical regions which are the regions where flicker effects are first perceived at the PJND level. To ensure the quality of data collected through crowdsourcing, we designed a robust framework that integrates our PJND assessment method and uses synthetic JND-critical regions as ground truth for training workers and worker reliability filtering. Our crowdsourcing experiment yielded a dataset of 300 source images and their compressed versions processed with JPEG or BPG, each annotated by 43 PJND ratings and 129 self-reported JND-critical regions. This dataset is named KonJND++ and will be made available online and provides valuable information for the field of image compression and quality assessment.

## REFERENCES

- [1] S. Stevens, "On the psychophysical law," in *Stevens' Handbook of Experimental Psychology*, vol. 2. John Wiley & Sons, 1957, pp. 742–787.
- [2] P. Manocha, A. Finkelstein, R. Zhang, N. J. Bryan, G. J. Mysore, and Z. Jin, "A differentiable perceptual audio metric learned from just noticeable differences," *arXiv preprint arXiv:2001.04460*, 2020.
- [3] H. Quené, "On the just noticeable difference for tempo in speech," *Journal of Phonetics*, vol. 35, no. 3, pp. 353–362, 2007.
- [4] J. S. Bradley, R. Reich, and S. Norcross, "A just noticeable difference in c50 for speech," *Applied Acoustics*, vol. 58, no. 2, pp. 99–108, 1999.
- [5] P. B. Nguyen, A. Beghdadi, and M. Luong, "Perceptual watermarking using a new Just-Noticeable-Difference model," *Signal Processing: Image Communication*, vol. 28, no. 10, pp. 1506–1525, 2013.
- [6] L. Jin, J. Y. Lin, S. Hu, H. Wang, P. Wang, I. Katsavounidis, A. Aaron, and C.-C. J. Kuo, "Statistical study on perceived JPEG image quality via MCL-JCI dataset construction and analysis," *Electronic Imaging*, vol. 2016, no. 13, pp. 1–9, 2016.
- [7] H. Lin, G. Chen, M. Jenadeleh, V. Hosu, U.-D. Reips, R. Hamzaoui, and D. Saupe, "Large-scale crowdsourced subjective assessment of picturewise just noticeable difference," *IEEE transactions on circuits and systems for video technology*, 2022.
- [8] H. Wang, I. Katsavounidis, J. Zhou, J. Park, S. Lei, X. Zhou, M.-O. Pun, X. Jin, R. Wang, X. Wang *et al.*, "VideoSet: A large-scale compressed video quality dataset based on JND measurement," *Journal of Visual Communication and Image Representation*, vol. 46, pp. 292–302, 2017.
- [9] X. Liu, Z. Chen, X. Wang, J. Jiang, and S. Kwong, "JND-Pano: Database for just noticeable difference of JPEG compressed panoramic images," in *Pacific Rim Conference on Multimedia*. Springer, 2018, pp. 458–468.
- [10] C. Fan, Y. Zhang, H. Zhang, R. Hamzaoui, and Q. Jiang, "Picture-level just noticeable difference for symmetrically and asymmetrically compressed stereoscopic images: Subjective quality assessment study and datasets," *Journal of Visual Communication and Image Representation*, vol. 62, pp. 140–151, 2019.
- [11] X. Shen, Z. Ni, W. Yang, X. Zhang, S. Wang, and S. Kwong, "Just Noticeable Distortion Profile Inference: A Patch-Level Structural Visibility Learning Approach," *IEEE Transactions on Image Processing*, vol. 30, pp. 26–38, 2020.
- [12] H. Wang, W. Gan, S. Hu, J. Y. Lin, L. Jin, L. Song, P. Wang, I. Katsavounidis, A. Aaron, and C.-C. J. Kuo, "MCL-JCV: a JND-based H. 264/AVC video quality assessment dataset," in *2016 IEEE International Conference on Image Processing (ICIP)*. IEEE, 2016, pp. 1509–1513.
- [13] L. Jin, J. Y. Lin, S. Hu, H. Wang, P. Wang, I. Katsavounidis, A. Aaron, and C.-C. J. Kuo, "Statistical study on perceived JPEG image quality via MCL-JCI dataset construction and analysis," *Electronic Imaging*, vol. 2016, no. 13, pp. 1–9, 2016.
- [14] ISO/IEC, "Information technology – Advanced image coding and evaluation – Part 2: Evaluation procedure for visually lossless coding," 2015, number ISO/IEC 29170-2:2015.
- [15] H. Lin, M. Jenadeleh, G. Chen, U.-D. Reips, R. Hamzaoui, and D. Saupe, "Subjective assessment of global picture-wise just noticeable difference," in *2020 IEEE International Conference on Multimedia & Expo Workshops (ICMEW)*. IEEE, 2020, pp. 1–6.
- [16] V. Hosu, F. Hahn, I. Zingman, and D. Saupe, "Reported attention as a promising alternative to gaze in IQA tasks," in *PQS 2016: 5th ISCA/DEGA Workshop on Perceptual Quality of Systems*, 2016, pp. 117–121.
- [17] J. Y. Lin, L. Jin, S. Hu, I. Katsavounidis, Z. Li, A. Aaron, and C.-C. J. Kuo, "Experimental design and analysis of JND test on coded image/video," in *Applications of digital image processing XXXVIII*, vol. 9599. International Society for Optics and Photonics, 2015, p. 95990Z.
- [18] M. Jiang, S. Huang, J. Duan, and Q. Zhao, "SALICON: Saliency in Context," in *The IEEE Conference on Computer Vision and Pattern Recognition (CVPR)*, June 2015.
- [19] V. Hosu, F. Hahn, I. Zingman, and D. Saupe, "Reported attention as a promising alternative to gaze in IQA tasks," in *PQS 2016: 5th ISCA/DEGA Workshop on Perceptual Quality of Systems*, 2016, pp. 117–121.
- [20] E. Pergament, P. Tandon, K. Tatwawadi, O. Rippel, L. Bourdev, B. Olshausen, T. Weissman, S. Katti, and A. G. Anderson, "An Interactive Annotation Tool for Perceptual Video Compression," *arXiv preprint arXiv:2205.03969*, 2022.
- [21] ISO 7810 ID-1, "Identification cards — Physical characteristics – Part 3.5: ID-1," 2019.
- [22] Q. Li, S. J. Joo, J. D. Yeatman, and K. Reinecke, "Controlling for participants' Viewing Distance in Large-Scale, psychophysical online experiments Using a Virtual chinrest," *Scientific Reports*, vol. 10, no. 1, pp. 1–11, 2020.
- [23] J. Le, A. Edmonds, V. Hester, and L. Biewald, "Ensuring quality in crowdsourced search relevance evaluation: The effects of training question distribution," in *SIGIR 2010 workshop on crowdsourcing for search evaluation*, vol. 2126, 2010, pp. 22–32.
- [24] Y. Cheng, "Mean shift, mode seeking, and clustering," *IEEE transactions on pattern analysis and machine intelligence*, vol. 17, no. 8, pp. 790–799, 1995.
- [25] Y. Patel, S. Appalaraju, and R. Manmatha, "Saliency driven perceptual image compression," in *Proceedings of the IEEE/CVF Winter Conference on Applications of Computer Vision*, 2021, pp. 227–236.
- [26] O. Wiedemann, V. Hosu, H. Lin, and D. Saupe, "Disregarding the big picture: Towards local image quality assessment," in *2018 Tenth International Conference on Quality of Multimedia Experience (QoMEX)*. IEEE, 2018, pp. 1–6.
- [27] V. Hosu, F. Hahn, O. Wiedemann, S.-H. Jung, and D. Saupe, "Saliency-driven image coding improves overall perceived JPEG quality," in *2016 Picture Coding Symposium (PCS)*. IEEE, 2016, pp. 1–5.
- [28] O. Wiedemann, V. Hosu, H. Lin, and D. Saupe, "Foveated video coding for real-time streaming applications," in *2020 Twelfth International Conference on Quality of Multimedia Experience (QoMEX)*. IEEE, 2020, pp. 1–6.